Overexpression of endoplasmic reticulum protein 29 regulates mesenchymal–epithelial transition and suppresses xenograft tumor growth of invasive breast cancer cells

I Fon Bambang[1,4], Songci Xu[1,4], Jianbiao Zhou[2], Manuel Salto-Tellez[1], Sunil K Sethi[1,3] and Daohai Zhang[1,3]

Endoplasmic reticulum protein 29 (ERp29) is a novel endoplasmic reticulum (ER) secretion factor that facilitates the transport of secretory proteins in the early secretory pathway. Recently, it was found to be overexpressed in several cancers; however, little is known regarding its function in breast cancer progression. In this study, we show that the expression of ERp29 was reduced with tumor progression in clinical specimens of breast cancer, and that overexpression of ERp29 resulted in G_0/G_1 arrest and inhibited cell proliferation in MDA-MB-231 cells. Importantly, overexpression of ERp29 in MDA-MB-231 cells led to a phenotypic change and mesenchymal–epithelial transition (MET) characterized by cytoskeletal reorganization with loss of stress fibers, reduction of fibronectin (FN), reactivation of epithelial cell marker E-cadherin and loss of mesenchymal cell marker vimentin. Knockdown of ERp29 by shRNA in MCF-7 cells reduced E-cadherin, but increased vimentin expression. Furthermore, ERp29 overexpression in MDA-MB-231 and SKBr3 cells decreased cell migration/invasion and reduced cell transformation, whereas silencing of ERp29 in MCF-7 cells enhanced cell aggressive behavior. Significantly, expression of ERp29 in MDA-MB-231 cells suppressed tumor formation in nude mice by repressing the cell proliferative index (Ki-67 positivity). Transcriptional profiling analysis showed that ERp29 acts as a central regulator by upregulating a group of genes with tumor suppressive function, for example, E-cadherin (*CDH1*), cyclin-dependent kinase inhibitor (*CDKN2B*) and spleen tyrosine kinase (*SYK),* and by downregulating a group of genes that regulate cell proliferation (eg, *FN*, epidermal growth factor receptor (*EGFR)* and plasminogen activator receptor (*uPAR*)). It is noteworthy that ERp29 significantly attenuated the overall ERK cascade, whereas the ratio of p-ERK1 to p-ERK2 was highly increased. Taken together, our results showed that ERp29 is a novel regulator leading to cell growth arrest and cell transition from a proliferative to a quiescent state, and reprogramming molecular portraits to suppress the tumor growth of MDA–MB–231 breast cancer cells.

Breast cancer recurrence is often found in patients after removal of the primary tumor and adjuvant therapy. For example, about 30–74% of breast cancer patients diagnosed at M0 or M1 tumor–node–metastasis tumor stages were found to have cancer cells in their bone marrow[1] and 20–45% of patients relapsed years or decades later.[2] Recent evidence suggests that tumor cells might disseminate at an early stage of tumor progression and evolve toward an aggressive phenotype in parallel with primary tumor.[3] Most of the disseminated cells are growth arrested at the G_0/G_1 phase and are characterized as quiescent dormant cells with high resistance to conventional chemotherapy.[4,5] However, the mechanisms that drive proliferative tumor cells to a quiescent state and activate survival signals in dormant cells are not fully understood.

[1]Department of Pathology, Yong Loo Lin School of Medicine, National University of Singapore, Singapore; [2]Cancer Science Institute of Singapore, Yong Loo Lin School of Medicine, National University of Singapore, Singapore and [3]Department of Laboratory Medicine, National University Hospital, Singapore
Correspondence: Dr D Zhang, PhD, Department of Laboratory Medicine, National University Hospital, 5 Lower Kent Ridge Road, Singapore 119074, Singapore.
E-mail: daohai_zhang@nuhs.edu.sg
[4]These authors contributed equally.

Tumor cell dormancy is driven by complicated mechanisms, including downregulation of u-plasminogen activator receptor (uPAR),[6] loss of $\beta1$ integrin[7] or inhibition of focal adhesion kinase (FAK),[8] and upregulation of p38 signaling.[9] The uPAR/$\alpha5\beta1$ integrin complex is essential for propagating mitogenic signals through the Ras/extracellular signal-regulated kinase (ERK) pathway by recruiting FAK and the EGF receptor (EGFR).[6] Disruption of the uPAR complex activates p38 mitogen-activated protein kinase (MAPK) signaling, which may exert tumor suppression functions on metastatic cells by causing cell growth arrest, senescence or apoptosis.[10] One of the mechanisms of p38-induced dormancy involves downregulation of JUN and inhibition of eukaryotic initiation factor-2α (eIF2α) activity.[11] In addition, endoplasmic reticulum (ER) stress signaling has a key role in tumor cell dormancy by way of activating RNA-dependent protein kinase-like ER kinase/phospho-eIF2α (PERK/p-eIF2α) signaling and inducing G_0/G_1 arrest.[12–14] These effects have been evidenced by the fact that the PERK pathway inhibits hyperproliferation of tumor cells and tumor formation.[15]

Endoplasmic reticulum protein 29 (ERp29), a novel reticuloplasmin, was first cloned from rat liver and enamel cells.[16,17] Structurally, it has an ER-retrieval signal of the C-terminal tetrapeptide (KEEL) targeting the ER lumen, but lacks the classical chaperone, disulfide-editing, calcium-buffer, and stress-response properties.[18] It has been shown that ERp29 is directly associated with the folding and/or secretion of thyroglobulin,[19] as well as resistance to oxidative and radiation stress.[20,21] Importantly, it was found to be highly expressed in primary tumor and cell lines.[22–24] Recent findings that ERp29 expression correlated with tumor growth rate[24] and knockdown of ERp29 by siRNA in noninvasive MCF-7 breast cancer cells attenuated tumorigenesis[25] imply an oncogenic role of ERp29 in breast tumor formation. In contrast, Shnyder *et al*.[24] also observed a low level of ERp29 in proliferative and metastatic MDA-MB-435 cells compared with MCF-7 cells, and an inverse correlation between ERp29 expression and tumor progression, although not at a significant level. Furthermore, expression of ERp29 was higher in the slow-growing tumors formed by MCF-7 or COLO 205 cell lines than in the fast-growing tumors produced by MDA-MB-435 or SW-620 cell lines. These phenomena may indicate a potential function of ERp29 in negatively regulating cell proliferation and/or tumorigenesis. In view of these controversial findings, the pathophysiological role of ERp29 in breast cancer progression remains elusive and needs to be further assessed.

This study aims at examining the functional consequences of ERp29 in breast cancer cells. Our study shows that ectopic expression of ERp29 in MDA-MB-231 cells results in G_0/G_1 arrest, causes mesenchymal–epithelial transition (MET) and suppresses tumor growth in nude mice. We show a tumor suppressive role of ERp29 by driving the molecular alterations in proliferative/invasive MDA-MB-231 cells.

MATERIALS AND METHODS

Reagents
Antibodies used include ERp29 (Acris, Hiddenhayse, Germany); E-cadherin (Stressgen, Victoria, Canada); fibronectin (FN), Akt, and pSer[473]-Akt (Cell Signaling Technology, Beverley, MD, USA); ERK and pTyr[204]-ERK (Santa Cruz Biotechnology, Santa Cruz, CA, USA); Vimentin (Millipore Corpaoration, Billerica, MA); and β-actin (Sigma-Aldrich, Steinheim, Germany). SuperSignal West Pico Chemiluminescent Substrate was from Pierce (Rockford, IL, USA). Geneticin (G418) was purchased from Invitrogen (Eugene, OR, USA).

Clinical Specimen and Cell Culture
In this study, 12 frozen breast tumor tissues and 12 adjacent nontumor breast tissues were obtained from the Tissue Repository of the Singapore National University Health System with informed patient consent. Usage of these tissues complied with the regulations set by our Institutional Review Board (IRB) for research purposes.

The MDA-MB-231, SKBr3, and MCF-7 human breast cancer cell lines were purchased from the American Type Culture Collection (ATCC, Manassas, VA, USA). Both MDA-MB-231 and MCF-7 cells were cultured in DMEM medium supplemented with 10% fetal bovine serum (FBS, Invitrogen) and were maintained at 37 °C with 5% CO_2 in a humidified incubator. SKBr3 cells were cultured in McCoy5A medium with 10% FBS. ERp29-transfected MDA-MB-231 and SKBr3 cells and shRNA/ERp29-transfected MCF-7 cells and their respective vector-transfected control cells were maintained in a medium supplemented with 10% FBS and G418 (2 mg/ml for MDA-MB-231 single clones, 0.5 mg/ml for SKBr3 mixed clones and 1 mg/ml for MCF-7 mixed clones).

Plasmids
The vector control plasmid, pcDNA3.1(+), was purchased from Invitrogen. The full-length cDNA of the human *ERp29* gene was amplified by PCR and cloned into pcDNA3.1(+) to form expression vector pcDNA-ERp29. The authenticity of the *ERp29* gene sequence was confirmed by DNA sequencing. A hairpin shRNA targeting *ERp29* (NM_006817) and a control shRNA targeting *EGFP* cDNA were constructed and cloned into pSilencer2.0-U6 (Ambion, Austin, TX, USA), as described in the Supplementary Materials and Methods.

Transfection and Generation of Stable Clones
For single clone generation, MDA-MB-231 cells (2×10^5 per well) seeded in 6-well plates were transfected with 1 μg of either pCDNA-ERp29 or pcDNA3.1 using LipofectAMINE (Invitrogen) according to the manufacturer's instructions. Transfectants were propagated in DMEM with G418 (2 mg/ml) for 48 h and then subcultured in Petri dishes after serial dilution. Colonies produced from single cells were detached in cloning cylinders (Millipore Corporation) and transferred into a 96-well plate for cell propagation. Two ERp29-over-

expressing single clones (clone B and clone E) showing different expression levels of ERp29 were used in this experiment. Transfection of SKBr3 cells with pCDNA-ERp29 or pcDNA3.1 and knockdown of ERp29 in MCF-7 cells by shRNA were performed following the same procedure. Both transfected SKBr3 cells (mixed clones) and MCF-7 cells (mixed clones) were cultured in McCoy5A medium with G418 (0.5 mg/ml) or DMEM medium with G418 (1.0 mg/ml) and used in this study. Cells transfected with vector pcDNA 3.1 or pshCtrl were used as a control. Expression of ERp29 was verified by reverse transcription-polymerase chain reaction (RT-PCR) and western blotting.

Cell Proliferation and Cell Cycle

Cell proliferation and cell cycle analysis were performed as described earlier.[26.] Briefly, cells (1×10^3 per well) were seeded in triplicate in 96-well culture plates and cultured for 4 days at 37 °C in a humidified, 5% CO_2 atmosphere. Viable cells were quantified at each 24-h interval using CellTiter 96[®;] Aqueous One Solution Cell Proliferation Assay (Promega, Mannheim, Germany). The absorbance at 492 nm was measured using an Infinite F200 microplate reader (TECAN Austria GmbH, Grodig, Austria). For cell cycle analysis, serum-starved cells were collected, fixed with ice-cold 80% ethanol for 1 h at 4 °C and stained with 1-ml propidium iodide/RNAase staining buffer (BD Biosciences, San Diego, CA, USA) for 1 h in the dark, followed by flow cytometric analysis (FACSCalibur, Becton Dickinson, Mansfield, MA, USA). The fraction of cells in each cell cycle phase (G_0/G_1, S and G2/M) was determined from the DNA histograms using Cyan LX software.

Cell Migration

Cell migration was assessed using wound healing and Transwell assays.[26] For wound healing assay, monolayer cells at 90–95% confluence were serum starved for 24 h and then carefully wounded using sterilized pipette tips. After removing detached cells, the cells were incubated at 37 °C for 15 h. Wound cells were photographed immediately ($t = 0$) and after being cultured for 15 h. Quantitative cell migration assays were performed using Cytoselect[TM] 24-Well Cell Migration Assay (Cell Biolabs, San Diego, CA, USA). Briefly, cells were serum starved for 24 h, harvested and seeded (7.5×10^5 cells/ml) in triplicate into the upper chambers. The inserts were then put into wells containing 0.5 ml of medium with 10% FBS, and incubated at 37 °C for 20 h in a 5% CO_2 incubator. Upon removal of nonmigratory cells with cotton swabs, migratory cells were stained and quantified at 570 nm, according to the provided protocol.

Matrigel Invasion

In vitro cell invasion was measured using QCM™ 24-Well Cell Invasion Assay (Chemicon International, Temecula, CA, USA) with an 8 μm pore size according to the manufacturer's instructions. Briefly, cells were serum starved for 24 h and

harvested. Equal number of cells (7.5×10^5 cells/ml) were seeded in triplicate onto the top of the Matrigel layer in the inserts and incubated at 37 °C for 24 h, with 10% FBS in the lower chamber. The cell suspension was aspirated and excess Matrigel was removed from the filter using cotton swabs. Cells at the bottom of the membrane were then dissociated with cell detachment buffer, and subsequently lysed and detected using CyQuant GR[®] dye. Relative cell invasion was determined on the basis of fluorescence reading at 485/ 535 nm.

Anchorage-Independent Growth in Soft Agar and Cell Transformation

Colony-forming efficiency in soft agar was performed using the CytoSelect™ 96-Well Cell Transformation assay (Cell Biolabs). Briefly, viable single cells (1×10^4) in 0.3% agar solutions were plated in triplicate over a layer of medium with 0.5% agar in a 96-well plate and incubated for 2 weeks in a humidified incubator at 37 °C with 5% CO_2. Colonies on the soft agar were photographed and transformed cells were lysed and detected using CyQuant Working Solution (Cell Biolabs) according to the manufacturer's protocol. Transformation efficiency was calculated according to the fluorescence reading at 485/535 nm.

Immunofluorescence and Confocal Microscopy

Immunofluorescence analysis was performed as described earlier.[26] Briefly, cells plated on coverslips were fixed with 4% paraformaldehyde (Sigma-Aldrich) for 20 min and permeabilized with 0.1% Triton X-100 for 10 min. The cells were then incubated overnight with primary antibodies against FN or E-cadherin or vimentin at 4 °C, followed by incubation with Alexa Fluor 488-conjugate streptavidin (1:2000, Invitrogen) for 1 h at room temperature. Actin filaments were stained with rhodamine-phalloidin (1:1000, Invitrogen) for 45 min. After the final washes with PBS, the coverslips were mounted using an antifade mounting fluid containing DAPI and images were examined and captured using an Olympus Fluoview FV500 confocal laser scanning microscope (Olympus, Japan). Raw images were analyzed using Olympus FV10-ASW 1.7 Viewer software (Olympus).

Western Blot Analysis

In all, 40 μg of protein was resolved by SDS-PAGE and transferred onto a PVDF membrane, and then probed with specific antibodies (ERp29, 1:2500; Akt, 1: 1000; p-Akt, 1:500; ERK, 1:1000; p-ERK, 1:500; E-cadherin, 1:200; and vimentin, 1:500). Goat-anti-mouse or goat-anti-rabbit IgG horseradish peroxidase (HRP, Upstate Biotechnology, Lake Placid, NY, USA) was used as secondary antibody. Chemiluminescent signals were visualized using SuperSignal West Pico Chemiluminescent Substrate (Pierce) and signal intensity was analyzed using GeneTools software (Syngene, Frederick, MD, USA). The level of β-actin was used as loading control.

Xenograft Studies

Cells (5×10^6) suspended in 0.1 ml of sterilized PBS buffer were mixed with 0.1 ml of high-concentration Matrigel (BD Biosciences) and injected subcutaneously (s.c.) into the mammary fat pad of female BALB/c athymic nude mice. Three female mice were injected with mock-transfected MDA-MB-231 control cells and six were injected with ERp29-transfected MDA-MB-231 cells (three for clone B and three for clone E). The kinetics of tumor growth were determined by measuring tumor volume (mm^3, V = tumor length × tumor width^2/2) every 2–3 days using calipers. Mice were killed and tumors were excised and kept in liquid nitrogen. The protocol was reviewed and approved by the Institutional Animal Care and Use Committee of the National University of Singapore. All animal experiments were carried out according to the guidelines on the care and use of animals for scientific purpose.

Tissue Microarray and Immunohistochemistry

Archival paraffin tissue blocks including 98 breast tumor and 98 adjacent nontumor breast tissues excised during the period 2000–2003 were retrieved from the Department of Pathology, National University Health System. The histopathological characteristics of these tumors were obtained from the Diagnostic Molecular Oncology Centre, National University Hospital. There were (i) 19 tumors with stage I, 50 with stage II and 29 with stage III–IV; (ii) 25 with pT1, 54 with pT2 and 19 with pT3–4; (iii) 56 with lymph node negative and 42 with lymph node positive; (iv) 36 with tumor size <2 cm and 62 with tumor size >2 cm; (v) 52 with HER-2/neu positive and 46 with HER-2/neu negative; (vi) 60 with ER positive and 38 with ER negative; and (vii) 56 with PR positive and 42 with PR negative. In all, 98 tumor and adjacent nontumor breast tissues were respectively arrayed on two paraffin blocks using a tissue-arraying instrument (Beecher Instruments, Silver Spring, MD, USA) at the Diagnostic Molecular Pathology Centre according to a similar procedure as described earlier.[27] Immunostaining of ERp29 was performed using the DAKO Envision$^+$ system (Dako, Glostrup, Denmark). Briefly, both tumor and nontumor tissue sections were blocked with 3% hydrogen peroxide after antigen unmasking with DAKO® Target Retrieval Solution in a microwave oven. Sections were incubated for 1 h with anti-ERp29 (1:500), followed by detection with labeled dextran polymer conjugated with peroxidase and DAB$^+$-substrate chromogen solution. The staining level was scored as negative (0), weak (1), moderate (2) and strong (3), according to the staining intensity of tumor cells. Tumors with a strong staining intensity of ERp29 were considered as high expression, while the others were considered as low expression. All sections were examined without previous knowledge of clinical information for any of the cases.

Proliferation Index and Cell Apoptosis in Mice Tumors

Frozen tumor tissues from mice were processed for paraffin block preparation using embedding molds. Paraffin sections were cut at 4 μm thickness and stained by hematoxylin and eosin (H&E). Immunohistochemical staining for ERp29 or Ki67 was carried out using the Dako Envision$^+$ system as described above. Slides were washed, counterstained with Mayer's hematoxylin and mounted. The staining intensity of ERp29 or Ki67 in tumor cells was assessed under light microscopy. Tumor cell apoptosis was assessed by evaluating TUNEL-positive cells using the DeadEnd Fluorometric TUNEL System (Promega, Madison, WI, USA). TUNEL staining was performed using TUNEL labeling mix according to the manufacturer's protocol (Supplementary Materials and Methods), and counterstained with DAPI. Fluorescence images were captured using an Olympus Fluoview FV500 confocal laser-scanning microscope (Olympus).

Real-Time PCR Array

Real-time PCR array analysis on the genes involved in the MAPK and PI3K/Akt pathway and cell invasion/metastasis was performed using the RT^2 Profiler™ PCR Array (SuperArray Bioscience Corporation, Frederick, MD, USA). Briefly, 0.5 μg of total RNA was used for first-strand cDNA synthesis using the RT^2 First Strand Kit according to the provided protocol. RT-PCR was carried out with the 96-well plate format and the ABI 7500 Fast Real-Time PCR System (Applied Biosystems, Singapore). Gene amplification was detected with SYBR, and data analysis was carried out using the ΔΔCt method (http://www.superarray.com/pctarraydataanalysis.php) according to the manufacturer's instructions. Relative expressions of genes were expressed as fold changes compared with control. Unsupervised hierarchical clustering was performed after filtered data were log$_2$ transformed using GeneSpring GX10.0 software, and results were shown using the TreeView program (Agilent Technologies, Santa Clara, CA, USA).

Reverse Transcription (RT)-PCR

Total RNA from cells was extracted using NucleoSpin RNA II (Macherey-Nagel GmbH & Co. KG, Germany), and cDNA was synthesized using ImProm-II reverse transcriptase (Promega) according to manufacturer's protocol. The genes of *ERp29, CDH1, CD82, EPHB2, CXCL12, ETV4, SYK, CCND2, CDKN2B, MAP4K1, uPAR* and *EGFR* were amplified by semiquantitative PCR using their respective specific primers (Supplementary Materials and Methods). *β*-Actin was used as loading control.
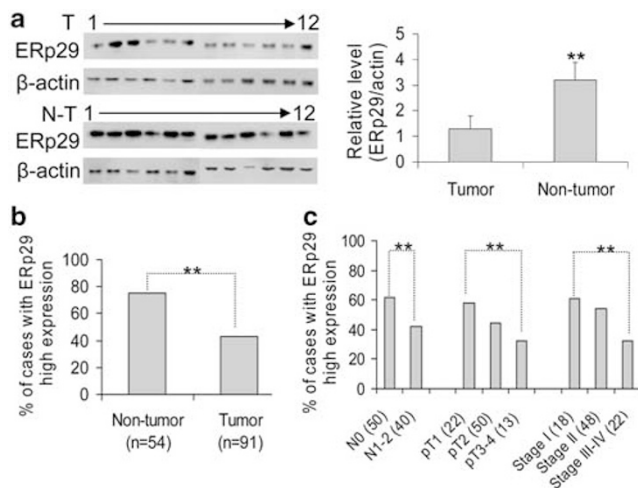
Statistical Analysis

All cell culture experiments were carried out in triplicate and repeated at least twice. One-way analysis of variance or Student's *t*-test was used to analyze the significance of differences. Two-tailed $P < 0.05$ was considered significant and data are presented as means ± s.d.

RESULTS

### Erp29 is Downregulated in Breast Carcinoma

We analyzed the expression pattern of ERp29 in 12 pairs of breast cancer tissues by immunoblotting. As shown in Figure 1a, the level of ERp29 is highly reduced in tumors when compared with a group of matched nontumor counterparts, suggesting a suppressive role of ERp29 in tumorigenesis. In the tissue array study, ERp29 was immunohistochemically stained and the level of ERp29 was assessed according to staining intensity. After immunohistochemical staining, 54 nontumor tissues and 91 tumor tissues were available for scoring. Representative IHC sections showing high and low staining intensity of ERp29 in both nontumor and tumor specimens are shown in Supplementary Figure 1. With these criteria, we found that ERp29 was highly stained in 75% of nontumor tissues ($n = 54$) and in 45% of tumor tissues ($n = 91$) ($P < 0.05$) (Figure 1b). We then investigated the correlation of ERp29 with the clinicopathological parameters of these tumors and found that ERp29 is highly expressed in a group of tumors with lower stage or lower grade or with lymph node negative when compared with tumors with more aggressive characteristics (Figure 1c). However, we did not observe significant associations of ERp29 with HER-2/neu and ER status (data not shown). We thus show that ERp29 expression is progressively repressed during cancer progression.

Erp29 Negatively Regulates Cell Proliferation in Breast Cancer Cells

To characterize the possible association of ERp29 with cell proliferation and/or invasive capability, we analyzed ERp29 expression in a panel of breast cell lines, including non-tumorigenic MCF-10A and MCF-12A cells, low-proliferative MCF-7 cells and high-proliferative MDA-MB-231, as well as SKBr3 and BT549 cells. As shown in Figure 2a, the level of ERp29 in high-proliferative cancer cells is highly reduced ($P < 0.05$) when compared with that in MCF-7 cells, which has the weakest invasive potential[28] and dormant characteristics.[29]
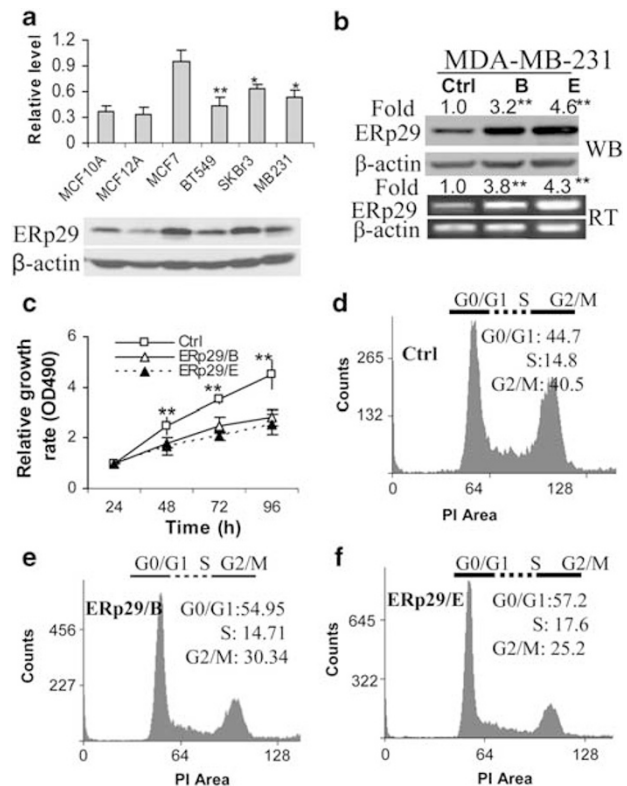
Figure 2 Expression of endoplasmic reticulum protein 29 (ERp29) in breast cancer cell lines and the effect on cell proliferation/cycle. (**a**) Expression of ERp29 in a subset of breast cell lines. ERp29 is reduced in high-proliferative breast cancer cell lines when compared with MCF-7. β-actin is used as loading control. Column: mean; bars, s.d. (**b**) Expression of ERp29 in ERp29-transfected MDA-MB-231 cells. Note the selected stable clones (B and E) with a high level of ERp29 as assessed by western blotting (upper panel) and reverse transcription-polymerase chain reaction (RT-PCR) (lower panel). Relative expression of ERp29 in clone B and E is indicated as a fold change of control cells. (**c**) Overexpression of ERp29 on cell proliferation. The cell proliferation of both clone B and E is inhibited by ERp29 overexpression in MDA-MB-231 cells. Cell proliferation was assessed using CellTiter 96® Aqueous One Solution Cell Proliferation Assay (Promega). bars, s.d. (**d**) Representative cell cycle diagram of mock-transfected MDA-MB-231 control cells. (**e**) Representative cell cycle diagram of ERp29-transfected MDA-MB-231 clone B cells. (**f**) Representative cell cycle diagram of ERp29-transfected MDA-MB-231 clone E cells. Note the increased cell populations at the G_0/G_1 phase in both clone B and E cells when compared with control cells. * $P < 0.05$, ** $P < 0.01$ when compared with that of MCF-7 (**a**) and control cells (**b, c**).

Figure 1 Association of endoplasmic reticulum protein 29 (ERp29) expression with breast tumor progression. (**a**) Western blotting of ERp29 in breast tumor and nontumor tissues. The expression level of ERp29 was normalized to β-actin and is represented in the right panel. (**b**) Quantification of ERp29 expression by immunohistochemical analysis. In all, 91 tumor tissues and 54 nontumor tissues were assessed and the percentage of ERp29 highly stained cases in each group is depicted. (**c**) Distribution of ERp29 highly stained cases with tumor characteristics. High expression of ERp29 is mostly found in tumors with lymph node negative, stage I and/or pT1. ** indicates significant difference (one-way analysis of variance).

To test whether ERp29 negatively regulates cell proliferation/invasion, we established two single clones of ERp29-transfected MDA-MB-231 cells after serial dilution and propagation in medium with G418. Increased expression of ERp29 in these two clones was verified by RT-PCR and western blotting (Figure 2b). As indicated in Figure 2c, ERp29 overexpression significantly inhibited cell growth of both clone B and E. Cell cycle analysis showed that overexpression of ERp29 highly increased the proportion of G_0/G_1 cells and decreased the proportion of G2/M cells in both ERp29-transfected clone B (Figure 2e) and clone E (Figure 2f). Cell apoptosis analysis using the DeadEnd Fluorometric TUNEL System (Promega) (Supplementary Materials and Methods) supported that ERp29 did not increase cell death in MDA-MB-231 cells (Supplementary Figure 2). Furthermore, we also established ERp29-transfected mixed clones in SKBr3 cells and shRNA/ERp29-transfected mixed clones in MCF-7 cells. We showed that overexpression of ERp29 in SKBr3 attenuated cell growth, whereas knockdown of ERp29 in MCF-7 cells accelerated cell growth (Supplementary Figure 3). Taken together, the data indicate that ERp29 negatively regulates cell growth in breast cancer cells.

Erp29 Regulates Mesenchymal–Epithelial Transition in MDA-MB-231 Cells

We observed an important change of cell morphology induced by ERp29 in MDA-MB-231 cells. As shown in Figure 3a, mock-transfected control cells show a spindle-like fibroblastic morphology, whereas ERp29-transfected MDA-MB-231 cells (clone B and E) show a cobble-stone-like phenotype, which is identical to that observed in dormant MCF-7 cells. We also observed that ERp29-transfected MDA-MB-231 cells grew to form clusters, whereas mock-transfected control cells grew sparsely when cells were cultured in flasks (Supplementary Figure 4). Phalloidin staining further verified a significant difference in the cell shape and distribution of F-actin, implying that ERp29-transfected MDA-MB-231 cells underwent cytoskeletal reorganization with loss of filamentous stress fibers and cortical actin formation (Figure 3b). Concomitantly, the extracellular matrix (ECM) component FN, which is involved in cell transition from quiescence to proliferation,[29] was decreased in ERp29-transfected MDA-MB-231 cells, as shown by immunofluorescent staining (Figure 3c). Importantly, we observed that epithelial cell marker E-cadherin was highly expressed in

both clone B and E cells and its membranous distribution is identical to that observed in MCF-7 cells (Figure 3d). Meanwhile, the mesenchymal cell marker vimentin was highly reduced in both clone B and E (Figure 3e). RT-PCR and immunoblotting analyses further showed the transcriptional reactivation of E-cadherin by ERp29 (Figure 3f). We also examined the expression of Twist, a transcription factor that negatively regulated E-cadherin expression during epithelial–mesenchymal transition (EMT),[30] and verified its reduced expression in both the ERp29-transfected clones (Figure 3f, right panel). In addition, when ERp29 was silenced in MCF-7 cells, the level of vimentin was increased, whereas the level of E-cadherin was decreased, as assessed by immunofluorescent staining (Supplementary Figure 5), further showing that downregulation of ERp29 promotes EMT. In short, with the loss of mesenchymal cell marker vimentin and reactivation of E-cadherin in ERp29-transfected MDA-MB-231 cells, we conclude that ERp29 negatively regulates the EMT process in breast cancer cells.

Overexpression of Erp29 Reduces Cell Motility, Invasion, and Transformation

Epithelial–mesenchymal transition is a central process implicated in cancer invasion and metastasis.[31,32] ERp29-mediated MET may negatively regulate cell migration and invasion. In line with this notion, we found that the wound healing abilities of ERp29-transfected MDA-MB-231 cells (clone B and E) are markedly repressed, compared with those observed in mock-transfected control cells (Figure 4a). In contrast, knockdown of ERp29 in MCF-7 cells increased wound healing capacity. Quantitative analysis using Transwell chamber further showed the reduced cell motility of ERp29-transfected MDA-MB-231 ($P < 0.01$) and the increased migration of ERp29-silenced MCF-7 cells ($P < 0.05$, Figure 4b). In addition, ERp29 significantly decreased the invasive capacity of MDA-MB-231 cells ($P < 0.05$), although knockdown of ERp29 by shRNA in MCF-7 cells improved cell invasive capacity ($P < 0.05$, Figure 4c). Similar results were also observed in ERp29-transfected SKBr3 cells, in which overexpression of ERp29 reduced cell migration and invasion (Supplementary Figure 6a, b). As such, these results show that ERp29 negatively modulates cell migration and invasion in breast cancer cells.

Given that the colony-forming capacity of mammalian cells in soft agar correlates with their tumorigenic potential,[32]

Figure 3 Phenotypic change, cytoskeletal reorganization and expression of epithelial/mesenchymal markers. (**a**) Cell morphology. Cells were viewed under light microscope and photographed with digital camera. Endoplasmic reticulum protein 29 (ERp29)-transfected clone B and E cells show similar cell morphology to MCF-7 cells. Original magnification: × 40. (**b**) Distribution of F-actin. Cells on glass coverslips were stained with rhodamine-phalloidin for F-actin. Arrows indicate the distribution of F-actin. Note the loss of actin stress fibers and formation of cortical F-actin in the ERp29-transfected MDA-MB-231 clone B and E cells, identical to that observed in MCF-7 cells. (**c**) Immunofluorescence of fibronectin (FN). Expression of FN is strongly inhibited in both clone B and E. (**d**) Reexpression of E-cadherin in clone B and E. Expression pattern of E-cadherin in clone B and E is similar to that in MCF-7 cells. (**e**) Loss of mesenchymal cell marker vimentin in clone B and E. (**f**) Reverse transcription-polymerase chain reaction (RT-PCR) and western blotting of E-cadherin: Note that E-cadherin was upregulated, whereas transcription factor twist was downregulated in ERp29-transfected MDA-MB-231 cells. β-actin was used as loading control. DAPI (blue) was used for nuclear staining. Original magnification: × 60.

we assessed the effect of ERp29 on the malignant properties of MDA-MB-231, SKBr3 and MCF-7 cells and found that ERp29-transfected MDA-MB-231 cells (Figure 5a) and SKBr3 cells (Supplementary Figure 6c) produced fewer colonies and/or smaller sized colonies than did control cells. Conversely, knockdown of ERp29 stimulated colony formation in MCF-7 cells (Figure 5a, right panel). Quantitative determination of transformed cells further showed an inhibitory
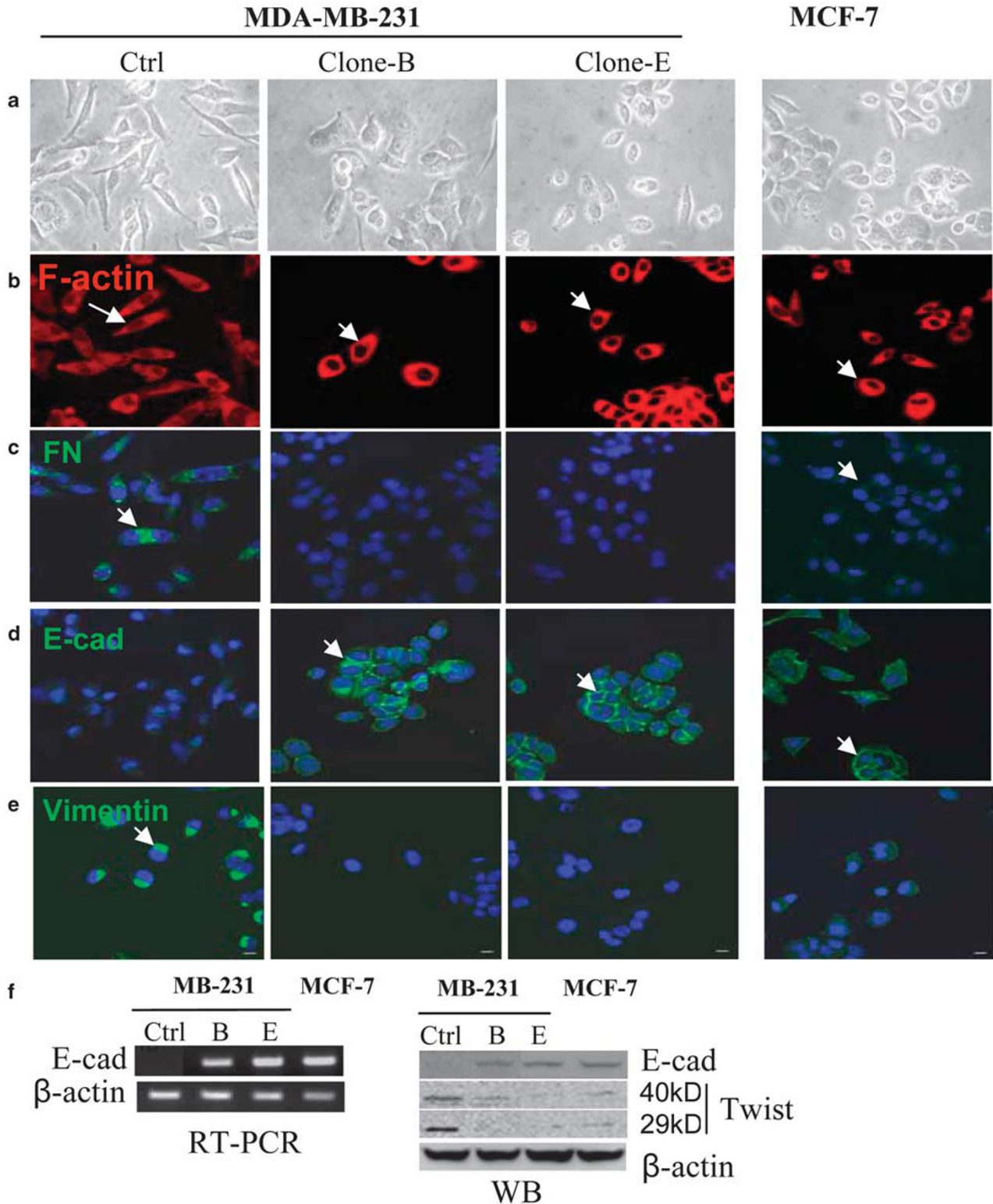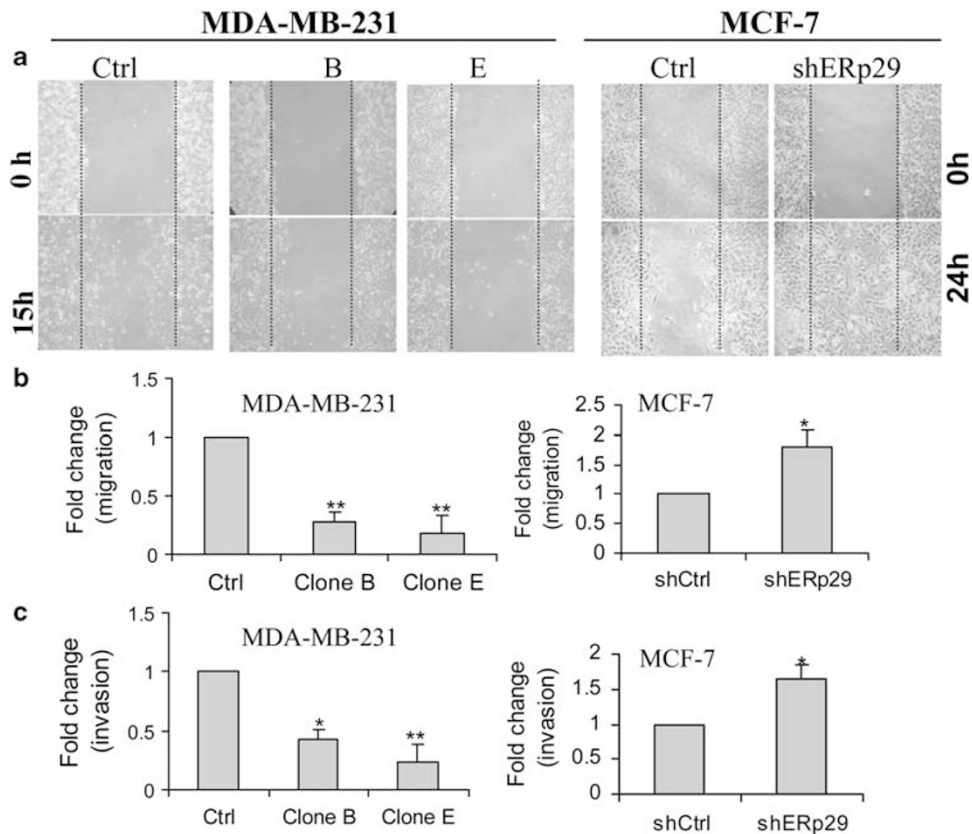
Figure 4 Endoplasmic reticulum protein 29 (ERp29) overexpression reduces cell migration and invasion. (a) Wound healing. Monolayer cells were wounded and photographs were taken immediately after wound induction and 15 h (or 24 h for MCF-7) later. (b) Migration through Transwell. Migration was performed as described in Materials and Methods. Migratory cells at the bottom of the membrane were stained and quantified at 570 nm, according to the provided protocol. Overexpression of ERp29 in clone B and E reduces cell motility, whereas silencing of ERp29 in MCF-7 stimulates cell motility. (c) Invasion through Matrigel. Cells invaded through Matrigel and attached to the bottom of the membrane were lysed and detected by CyQuant GR® dye. Relative cell invasion was determined from fluorescence reading at 485/535 nm. Note that ERp29 negatively regulates breast cancer cell invasion. Cell migration and invasion were expressed as a mean of fold change from three independent experiments compared with their respective control cells. Bars, s.d.; $*P < 0.05$; $** P < 0.01$.

effect of ERp29 on cell transformation in MDA-MB-231 (Figure 5b, left panel), MCF-7 (Figure 5b, right panel) and SKBr3 cells (Supplementary Figure 6c).

Erp29 Suppresses Tumor Formation In Vivo
We then investigated the effect of ERp29 on tumor growth in a xenograft model. We observed that all the mice injected with control cells showed visible tumors within 21 days after inoculation (mean = 30.8 mm³, $n = 3$), and the tumors grew aggressively up to 710 mm³ (mean) when mice were killed at day 48 (Figure 5c). In contrast, the onset of tumors in mice injected with ERp29-transfected MDA-MB-231 cells (clone B and E) was delayed and smaller nodules were observed (mean = 53.0 mm³, $n = 3$ of each clone) on day 48. ERp29-transfected MDA-MB-231 cells produced slow-growing tumors and the tumor sizes are smaller than those formed by control cells. To understand whether a high expression

of ERp29 was present in the killed tumors, we carried out immunohistochemical staining on formalin-fixed, paraffin-embedded tumor sections. As shown in Figure 6a, ERp29 was highly stained in ERp29-transfected tumor cells, compared with the tumors formed by mock-transfected control cells. Histological analysis indicated that both types of tumors were poorly differentiated carcinoma on the basis of the morphological characteristics of H & E stained sections (Figure 6b), with a minor area of central necrosis and a similar degree of tumor cell density (data not shown). To quantitatively compare the proliferation and apoptotic index of transfectant cell populations in developed tumors, tumor sections were stained for cell proliferation with Ki67 and for DNA fragmentation with TUNEL assay. Both the proliferation and apoptotic indexes were calculated from five randomly selected microscopic fields of each tumor section. We observed that the percentage of proliferating cells was dramatically
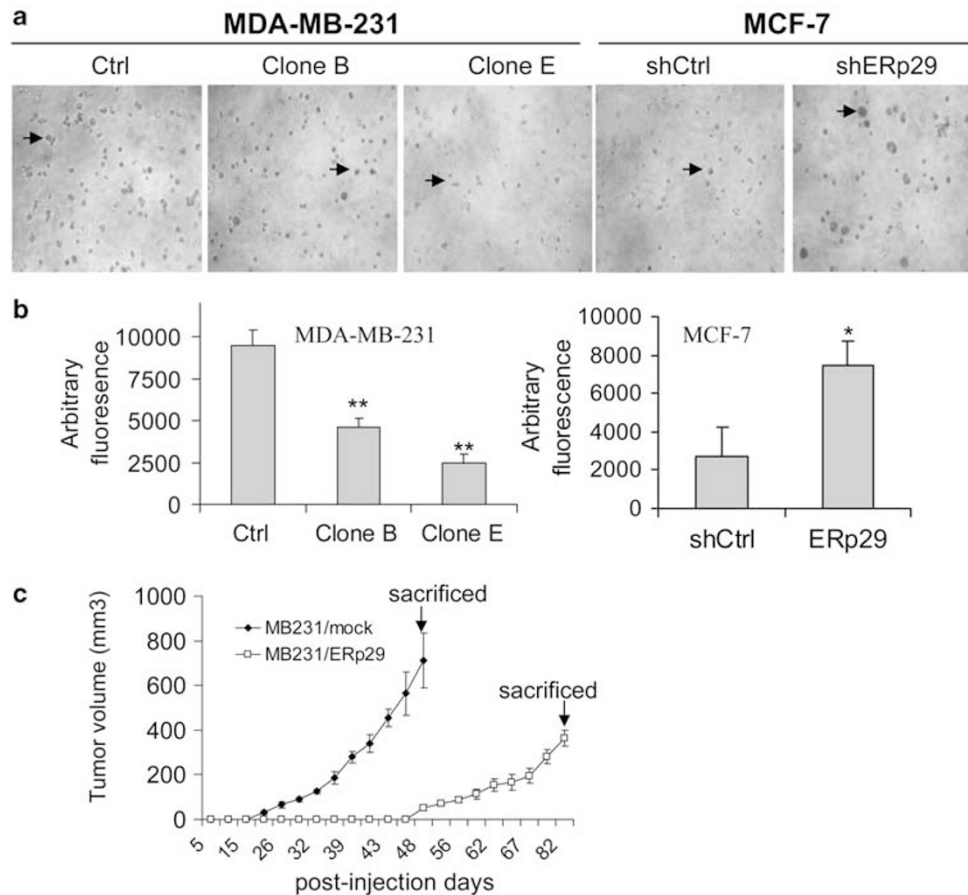
Figure 5 Endoplasmic reticulum protein 29 (ERp29) inhibits anchorage-independent colony formation in soft agar and *in vivo* tumor growth. (**a**) Colony formation. Equal numbers of viable cells were seeded on the top layer of soft agar and cultured for 2 weeks at 37 °C in a CO_2 (5%) incubator. Colonies on the soft agar were photographed under light microscope at × 20 magnification. Note the reduced number and/or size of colonies in clone B and E, and increased number and/or size of colonies in ERp29-silenced MCF-7 cells. (**b**) Quantitative analysis of cell transformation. Transformed cells were analyzed using CytoSelect Cell Transformation assay according to the manufacturer's protocol. Data represent the arbitrary value at 485/535 nm. Note that cell transformation is reduced in clones B and E and increased in ERp29-silenced MCF-7 cells. (**c**) Time of onset and rate of tumor progression in nude mice. Tumor size was measured until the animals were killed. ERp29 expression in clone B and E cells strongly inhibits tumor initiation and growth. Data represent the average of tumor size from the control group (mock-transfected MDA-MB-231 cells, $n = 3$) and the test group (ERp29-transfected cells, $n = 6$, 3 of each clone); *Column*, mean; *bars*, s.d. * $P < 0.05$; ** $P < 0.01$.

decreased in tumors produced by clone B or E of ERp29-transfected cells (Figure 6c). TUNEL staining indicated that no significant difference of apoptotic cells was found in tumors developed from ERp29-transfected cells as compared with that from control tumor cells (Figure 6d). These results suggest that the reduction in the cell proliferation rate of ERp29-transfected MDA-MB-231 cells is responsible for tumor suppression *in vivo*.

Identification of Erp29-Regulated Genes Involved in Cell Proliferation and Invasion

Our investigation reveals that overexpression of ERp29 in MDA-MB-231 cells results in MET and in reduction of cell proliferation/invasion and tumorigenesis. Given that MAPK/

ERK and PI3K/Akt signaling pathways have been hyperactivated in EMT,[33,34] we examined whether these two cascades were negatively regulated by ERp29 during ERp29-mediated MET. To this end, we performed RT-PCR array-based gene expression profiling by targeting MAPK and PI3K/Akt signaling pathways, as well as the genes involved in tumor invasion/metastasis. In all, 125 of 252 genes were differentially transcribed (by > 2.0 fold) in both ERp29-transfected clone B and E cells. Of them, 59 were upregulated, whereas 66 were downregulated (Supplementary Table 1). The unsupervised clustering of these genes was shown in Supplementary Figure 7 and the genes showing at least 10-fold difference are indicated in Figure 7a. We found that ERp29 could activate the transcription of a group of genes involved in tumor suppression (eg, *SYK*, *CDH1*, etc) and cell
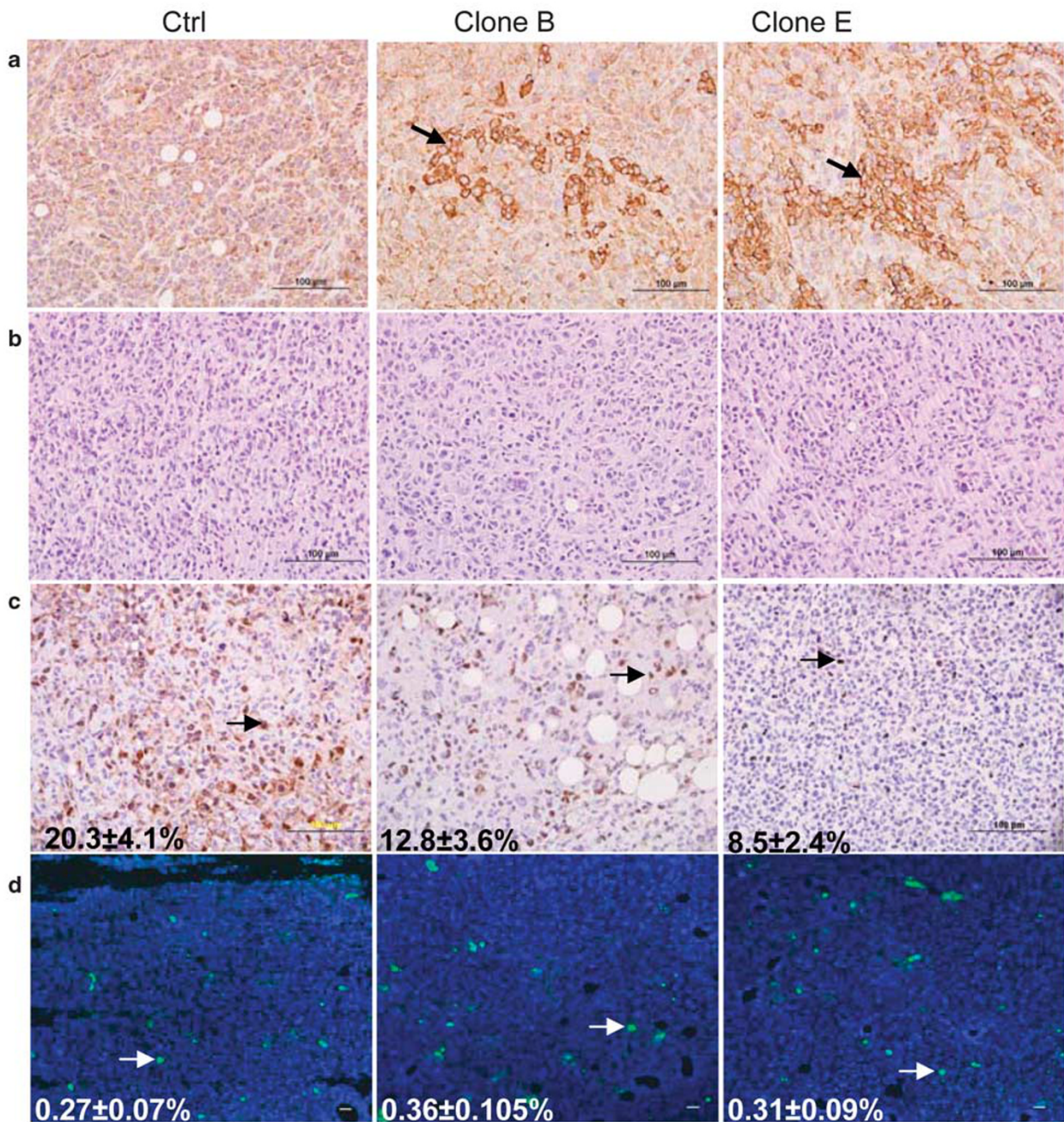
Figure 6 Immunohistochemical and TUNEL analysis of tumors developed from mice. (**a**) Representative immunostained sections stained with an antibody against endoplasmic reticulum protein 29 (ERp29). Arrows indicate cells showing high expression of ERp29 in tumors developed from ERp29-transfected clone B and E cells. (**b**) Representative H & E-stained sections. Formalin-fixed, paraffin-embedded sections were cut at 4 μm thickness and stained with H & E. (**c**) Representative tumor sections stained with an antibody against cell proliferation marker Ki-67. The number of Ki-67-positive cells was measured on sections of each tumor (five randomly selected fields per tumor section) and the mean of percentage of proliferating cells ± s.d. is indicated. Arrows indicate Ki-67-positive cells. (**d**) Cell apoptosis with TUNEL assay. Fragmented DNA of apoptotic cells was labeled with fluorescein-12-dUTP by Terminal Deoxynucleotidyl Transferase (rTdT) and visualized by fluorescence microscopy. The number of fluorescent cells (green, as indicated by arrows) was measured and the mean of the percentage of apoptotic cells was determined using the similar method as that for Ki-67.

cycle inhibition (eg, *CDKN2B*), and inhibit the transcription of a group of genes involved in cell proliferation (eg, *CCND$_2$*, *uPAR*, *EGFR*, *Akt*, etc) and oncogenesis (eg, proto-oncogene *MET* and invasion-related transcription regulator *ETV4*, etc). Activation of cyclin-dependent kinase inhibitor 2B (*CCKN2B*, p15), a G$_1$ checkpoint protein, and inhibition of *CCND$_2$* may indicate the
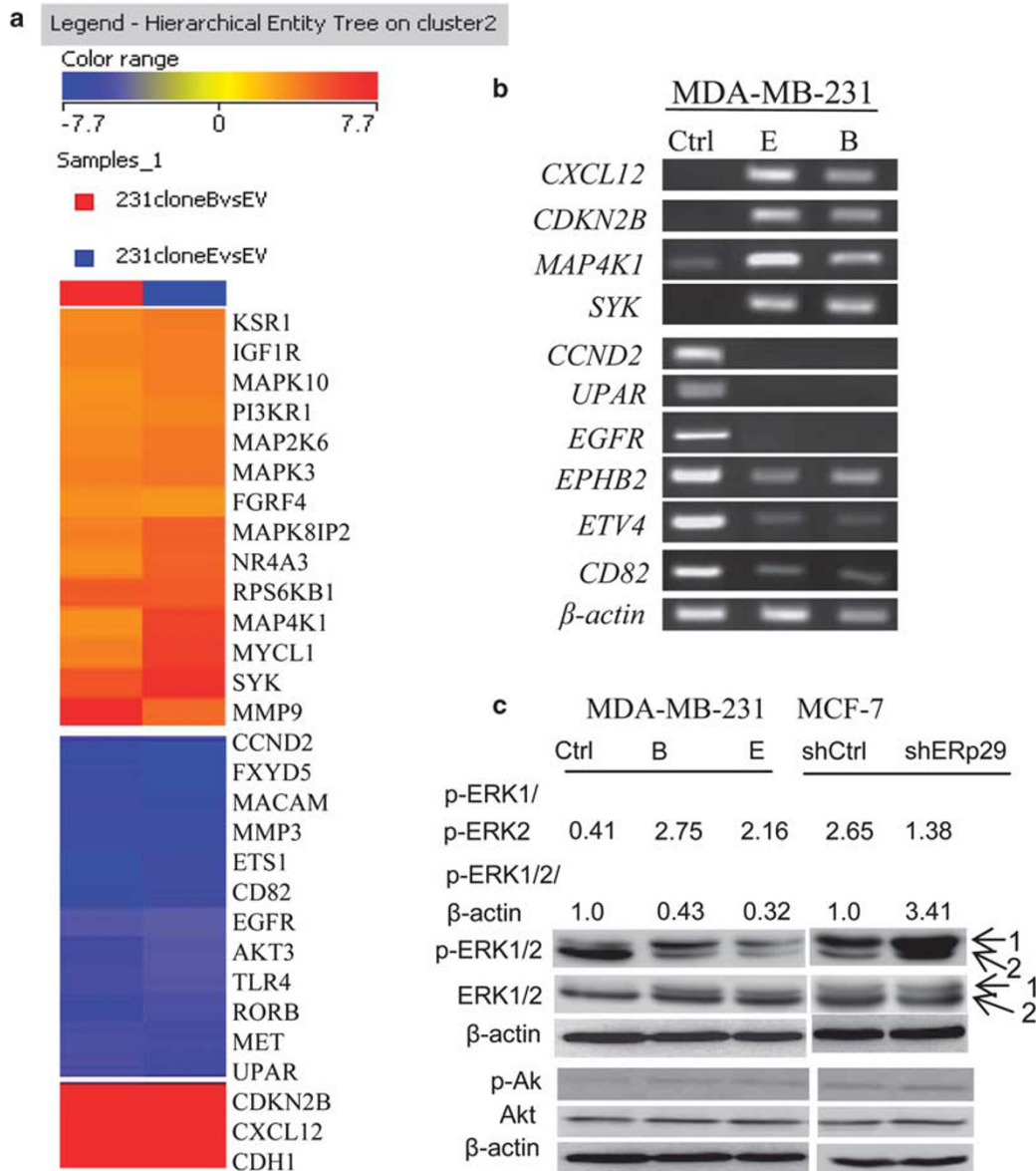
Figure 7 Unsupervised clustering of endoplasmic reticulum protein 29 (ERp29)-regulated genes involved in tumor invasion/metastasis, MAPK and PI3K/Akt pathways. (**a**) Clustering and identification of differentially expressed genes in the ERp29-transfected clone B and E. The genes showing at least 10-fold difference are highlighted. (**b**) Semiquantitative reverse transcription-polymerase chain reaction (RT-PCR)of differentially expressed genes. Four upregulated genes (*CXCL12, SYK, CDKN2B and MAP4K1*) and six downregulated genes (*CCND2, uPAR, EPHB2, EGFR, CD82* and *ETV4)* by ERp29 were validated by RT-PCR using their respective gene-specific primer sets. β-actin was used as loading control. (**c**) Inhibition of the MAPK, not the PI3K/Akt pathway, by ERp29. Activation of the ERK cascade is strongly reduced in ERp29-transfected clone B and E, and highly stimulated in ERp29-silenced MCF-7 cells. Total phosphorylation level was determined as a value of ratio (p-ERK1/2 to β-actin) after normalized to that in control cells (value set as 1.0). Note the negative regulation of ERp29 on total ERK cascade and the differential regulation of ERK1 and ERK2. Data represent the average from three independent experiments.

molecular basis of ERp29-mediated cell growth inhibition by causing G_0/G_1 arrest in ERp29-transfected MDA-MB-231 cells (Figure 2). In the MAPK cascade, *MAP4K1, MAP2K6, MAPK81P2, MAPK3* and *MAPK10* were transcriptionally upregulated, whereas *MAPK12/13/14, MAPK8* and *MAP2K3* were downregulated. Several important transcriptional factors (eg, *Ets-1* and *E2F*) were also transcriptionally repressed by ERp29. Meanwhile, transcription of the regulatory subunit of *PI3K* (*PI3KR1* and *PI3KR2*) and *Akt1* was increased, whereas transcription of the catalytic subunit of *PI3K* (*P3KCG*) and *Akt3* was reduced by ERp29 (Supplementary Table 1). RT-PCR further verified the differential expression of upregulated (*SYK, CDKN2B, MAP4K1* and *CXCL12)* and downregulated genes (*CCND2, UPAR, EGFR, EPHB2, CD82* and *ETV4*) in ERp29-transfected MDA-MB-231 cells (Figure 7b).

In addition to the transcriptional activation/inhibition of genes regulating invasion/metastasis and MAPK and PI3K cascades, overexpression of ERp29 in MDA-MB-231 cells significantly increased both expression and phosphorylation of ERK1 (MAPK3), and highly inhibited the phosphorylation of ERK2 (MAPK1), whereas the overall phosphorylation of p-ERK1/2 was reduced in ERp29-transfected clone B and E cells (Figure 7c). When ERp29 was silenced in MCF-7 cells, both ERK1 and two were highly phosphorylated, whereas the basal level of ERK1/2 was not changed (Figure 7c). Interestingly, we also found that ERp29 differentially regulated the phosphorylation of ERK1 and ERK2. The ratio of p-ERK1 to p-ERK2 was highly increased in ERp29-transfected clone B and E cells and was highly decreased in ERp29-silenced MCF-7 cells. These results indicated that ERp29 may regulate MAPK signaling by tuning the ratio of p-ERK1 to p-ERK2. However, phophorylation of Akt was only slightly increased, indicating a less effectiveness of ERp29 in regulating the overall activation of the PI3K/Akt cascade (Figure 7c). In general, our results show that ERp29 is a central molecule in modulating signal pathways at both transcriptional and translational levels.

DISCUSSION

Recent studies have established the key roles of major reticuloplasmins, including Bip/GRP78, PDI and other ER stress molecules (eg, PERK and p-eIF2α) in cancer cell apoptosis, survival and tumorigenesis.[15,35–37] In this study, we show that ERp29 is a novel regulator in modulating cell growth arrest and phenotypic changes associated with MET in proliferative/invasive breast cancer cells. Importantly, we show that ERp29 is a potential tumor suppressor in breast cancer progression.

We reported here that ERp29 exerts a growth-inhibitory effect in breast cancer cells. This was supported by our findings that overexpression of ERp29 in the proliferative MDA-MB-231 cells and SKBr3 cells significantly attenuated cell growth, whereas silencing ERp29 in low proliferative MCF-7 cells enhanced cell growth. We observed that the reduced cell proliferation in proliferative MDA-MB-231 cells was caused by the ERp29-mediated cell cycle arrest at the G_0/G_1 phase (Figure 2). In keeping with this, we found that key cell cyclins at the G_0/G_1 phase, for example, *CCND1, CCND2* and *CCND3,* were highly downregulated, whereas inhibitor *CDKN2B* was significantly upregulated in ERp29-transfected MBA-MD-231 cells, as assessed by RT-PCR-array (Figure 7b, Supplementary Table 1). Considering that ER stress signaling PERK/p-eIF2α has an essential role in regulating G_0/G_1 arrest by deregulating cyclin D1/D2,[13] it is meaningful to investigate the mechanism by which ERp29 regulates ER stress signaling and thereby cell cycle arrest.

A novel finding of our study is that ERp29 regulates cytoskeleton reorganization and MET transition in MDA-MB-231 cells (Figure 3). As the cell shape and cytoskeletal configuration have a critical role in regulating the transition of cells from a nonproliferative to a proliferative state,[4,29,38] the ERp29-mediated cytoskeletal reorganization in proliferative MDA-MB-231 cells indicated ERp29 as a novel regulator in inducing cell dormancy. This is further supported by the identical phenotype between ERp29-transfected MDA-MB-231 cells and dormant MCF-7 cells. Repression of a cell proliferation regulator FN[29] in ERp29-transfected MDA-MB-231 cells further supports the role of ERp29 in driving proliferative cells into a quiescent state. Accompanying the phenotypic change, we showed that E-cadherin, a key component of adherens junctions with a crucial role in the maintenance of epithelial integrity,[39] was transcriptionally activated and highly expressed in ERp29-transfected MDA-MB-231 cells by downregulating the transcriptional factor twist (Figure 3f). Given that E-cadherin expression inhibited the EMT process,[40] reactivation of E-cadherin and loss of mesenchymal cell marker vimentin in ERp29-transfected MDA-MB-231 cells suggest that these transfected cells undergo MET. Although the basis of ERp29-mediated MET transition in proliferative/invasive breast cancer cells remains elusive, we report, for the first time, that ERp29 is a novel regulator in modulating MET in invasive breast cancer cells.

This study shows ERp29 as a novel tumor suppressive factor in breast cancer. Increased expression of ERp29 inhibited cell migration, invasion and transformation *in vitro* in ERp29-transfected MDA-MB-231 and SKBr3 cells and *vice versa* in ERp29-silenced MCF-7 cells. Importantly, we confirmed that expression of ERp29 in proliferative MDA-MB-231 cells significantly delayed tumor initiation and dramatically inhibited tumor growth in a nude mice xenograft model, with a decreased cell proliferative index. The observed *in vivo* tumor suppression is consistent with our results with clinical samples: ERp29 is downregulated in tumors when compared with nontumor tissues and progressively reduced with tumor progression. In support of our findings, studies from Shnyder *et al.*[24] showed that cells (MCF-7 and COLO205) with a high level of ERp29 produced slow-growing tumors, whereas cells (MDA-MB-435) with a low level of ERp29 developed fast-growing tumors. Nevertheless, conflicting results have been reported by Mkrtchian *et al.*[25] They found that mutant ERp29C157A inhibited tumor growth as compared with wild-type ERp29, and the size of established tumors could not be further increased when tumors were treated with ERp29 siRNA. Although the reasons of this discrepancy are uncertain, one possible explanation may be that tumor suppression by nonfunctional mutant ERp29C157A is apparently because of the disruption of a secretion pathway,[41] which may affect stromal–tumor cell interaction. There is no further evidence to show that mutation of C157A could result in molecular alterations, which exert tumor suppressive capacity. In contrast, our *in vitro* and *in vivo* studies, together with the observations in the clinical specimen, established the tumor suppressive function of ERp29 in breast cancer.

The mechanisms by which ERp29 suppresses tumor growth are not fully understood; however, ERp29-mediated cell growth arrest, not cell apoptosis, and ERp29-driven MET transition, which enables cells to lose their invasive and metastatic properties,[31] may provide an insight into this process. In addition, the gene expression profiling analysis revealed a complexity of differentially expressed genes that may be involved in the tumor suppressive effect of ERp29 in breast cancer cells. For example, tumor suppressor genes (eg, *CDH1* and *SYK*) were transcriptionally activated and highly expressed, whereas the genes regulating cell proliferation (eg, *uPAR*, *FN* and *EGFR*) were significantly reduced in ERp29-transfected MDA-MB-231 cells (Supplementary Table 1, Figure 7). E-cadherin suppressed tumor formation by preventing genomic instability,[42] whereas SYK negatively regulated cell proliferation, invasion and tumor formation.[43] EGFR and uPAR were found to positively regulate cell migration, invasion and tumorigenesis.[44,45] Furthermore, the genes involved in MAPK and PI3K pathways are transcriptionally regulated and the overall activation of ERK cascade is inhibited by ERp29. The reduced ERK1/2 cascade in ERp29-transfected MDA-MB-231 cells further supports the involvement of ERK cascade in regulating EMT.[34,46] In addition to the overall reduction of p-ERK1/2, p-ERK1 and p-ERK2 were differentially regulated, whereby p-ERK1 was enhanced and p-ERK2 was attenuated in ERp29-transfected MDA-MB-231 cells (Figure 7c). Given that ERK1, which could antagonize ERK2 signaling, negatively modulates colony formation and tumorigenesis in nude mice,[47] the ERp29-enhanced ratio of p-ERK1/p-ERK2 may imply a novel regulatory model in determining ERp29-mediated ERK signaling activity and in driving their apparent biological differences.

In summary, we show that ERp29 negatively regulates cell growth by causing G_0/G_1 arrest. Importantly, we report a novel function of ERp29 in modulating MET transition by transcriptional activation of E-cadherin and in suppressing tumorigenesis through a complexity of molecular alterations. These findings provide a novel insight into the involvement of ERp29 in breast cancer progression. Future studies will examine ERp29-regulated genome-wide downstream signals to elucidate the molecular mechanisms underlying the phenotypic and pathological characteristics, and to investigate its involvement in metastasis using *in vivo* animal models.

1. Braun S, Vogl FD, Naume B, et al. A pooled analysis of bone marrow micrometastasis in breast cancer. N Engl J Med 2005;353: 793–802.
2. Karrison TG, Ferguson DJ, Meier P. Dormancy of mammary carcinoma after mastectomy. J Natl Cancer Inst 1999;91:80–85.
3. Schardt JA, Meyer M, Hartmann CH, et al. Genomic analysis of single cytokeratin-positive cells from bone marrow reveals early mutational events in breast cancer. Cancer Cell 2005;8:227–239.
4. Aguirre-Ghiso JA. Models, mechanisms and clinical evidence for cancer dormancy. Nat Rev Cancer 2007;7:834–846.
5. Naumov GN, Townson JL, MacDonald IC, et al. Ineffectiveness of doxorubicin treatment on solitary dormant mammary carcinoma cells or late-developing metastases. Breast Cancer Res Treat 2003;82:199–206.
6. Aguirre-Ghiso JA, Kovalski K, Ossowski L. Tumor dormancy induced by downregulation of urokinase receptor in human carcinoma involves integrin and MAPK signaling. J Cell Biol 1999;147:89–104.
7. Donald E, White DE, Kurpios NA, et al. Targeted disruption of β1-integrin in a transgenic mouse model of human breast cancer reveals an essential role in mammary tumor induction. Cancer cell 2004;6:159–170.
8. Aguirre-Ghiso JA. Inhibition of FAK signaling activated by urokinase receptor induces dormancy in human carcinoma cells *in vivo*. Oncogene 2002;21:2513–2524.
9. Ranganathan AC, Adam AP, Aguirre-Ghiso JA. Opposing roles of mitogenic and stress signaling pathways in the induction of cancer dormancy. Cell Cycle 2006;5:1799–1807.
10. Bulavin DV, Fornace AJ. P38 MAPK kinase's emerging rile as a tumor suppressor. Adv Cancer Res 2004;92:95–118.
11. Ranganathan AC, Zhang L, Adam AP, et al. Functional coupling of p38-induced up-regulation of BiP and activation of RNA-dependent protein kinase-like endoplasmic reticulum kinase to drug resistance of dormant carcinoma cells. Cancer Res 2006;66:1702–1711.
12. Cullinan SB, Diehl JA. Coordination of ER and oxidative stress signaling: the PERK/Nrf2 signaling pathway. Int J Biochem Cell Biol 2006;38:317–332.
13. Brewer JW, Diehl JA. PERK mediates cell-cycle exit during the mammalian unfolded protein response. Proc Natl Acad Sci USA 2000;97:12625–12630.
14. Ranganathan AC, Adam AP, Zhang L, et al. Tumor cell dormancy induced by p38SAPK and ER-stress signaling: an adaptive advantage for metastatic cells? Cancer Biol Ther 2006;5:729–735.
15. Sequeira SJ, Ranganathan AC, Adam AP, et al. Inhibition of proliferation by PERK regulates mammary acinar morphogenesis and tumor formation. PLoS ONE 2007;2:e615.
16. Demmer J, Zhou C, Hubbard MJ. Molecular cloning of ERp29, a novel and widely expressed resident of the endoplasmic reticulum. FEBS Lett 1997;402:145–150.
17. Mkrtchian S, Fang C, Hellman U. A stress-inducible rat liver endoplasmic reticulum protein, ERp29. Eur J Biochem 1998;251: 304–313.
18. Mkrtchian S, Sandalova T. ERp29, an unusual redox-inactive member of the thioredoxin family. Antioxid Redox Signal 2006;8: 325–337.
19. Sargsyan E, Baryshev M, Szekely L, et al. Identification of ERp29, an endoplasmic reticulum lumenal protein, as a new member of the thyroglobulin folding complex. J Biol Chem 2002;277:17009–17015.
20. Zhang B, Wang M, Yang Y, et al. ERp29 is a radiation-responsive gene in IEC-6 cell. J Radiat Res (Tokyo) 2008;49:587–596.
21. Dukes AA, Van Laar VS, Cascio M, et al. Changes in endoplasmic reticulum stress proteins and aldolase A in cells exposed to dopamine. J Neurochem 2008;106:333–346.
22. Myung JK, Afjehi-Sadat L, Felizardo-Cabatic M, et al. Expressional patterns of chaperones in ten human tumor cell lines. Proteome Sci 2004;2:8.
23. Cheretis C, Dietrich F, Chatzistamou I, et al. Expression of ERp29, an endoplasmic reticulum secretion factor in basal-cell carcinoma. Am J Dermatopathol 2006;28:410–412.

24. Shnyder SD, Mangum JE, Hubbard MJ. Triplex profiling of functionally distinct chaperones (ERp29/PDI/BiP) reveals marked heterogeneity of the endoplasmic reticulum proteome in cancer. J Proteome Res 2008;7:3364–3372.

25. Mkrtchian S, Baryshev M, Sargsyan E, *et al*. ERp29, an endoplasmic reticulum secretion factor is involved in the growth of breast tumor xenografts. Mol Carcinog 2008;47:886–892.

26. Bambang IF, Lu D, Li H, *et al*. Cytokeratin 19 regulates endoplasmic reticulum stress and inhibits ERp29 expression via p38/XBP-1 signaling in breast cancer cells. Exp Cell Res 2009;315:1964–1974.

27. Zhang D, Salto-Tellez M, Putti TC, *et al*. Reliability of tissue microarrays in detecting protein expression and gene amplification in breast cancer. Mod. Pathol. 2003;16:79–84.

28. Mukhopadhyay R, Theriault RL, Price JE. Increased levels of alpha6 integrins are associated with the metastatic phenotype of human breast cancer cells. Clin Exp Metastasis 1999;17:325–332.

29. Barkan D, Kleinman H, Simmons JL, *et al*. Inhibition of metastatic outgrowth from single dormant tumor cells by targeting the cytoskeleton. Cancer Res 2008;68:6241–6250.

30. Kang Y, Massague J. Epithelial-mesenchymal transition: twist in development and metastasis. Cell 2004;118:277–279.

31. Thiery JP. Epithelial-mesenchymal transitions in tumour progression. Nature Rev Cancer 2002;2:442–454.

32. Elenbaas B, Spirio L, Koerner F, *et al*. Human breast cancer cells generated by oncogenic transformation of primary mammary epithelial cells. Genes Dev 2001;15:50–65.

33. Larue L, Bellacosa A. Epithelial-mesenchymal transitions in development and cancer: role of phosphatidylinositol 3′ kinase/AKT pathways. Oncogene 2005;24:7443–7454.

34. Javle MM, Gibbs JF, Iwata KK, *et al*. Epithelial-mesenchymal transition and activated extracellular signal-regulated kinase (p-ERK) in surgically dissected pancreatic cancer. Ann Surg Oncol. 2007;14:3527–3533.

35. Li J, Lee AS. Stress induction of GRP78/BiP and its role in cancer. Curr Mol Med 2006;6:45–54.

36. Raught B, Gingras AC, James A, *et al*. Expression of a translationally regulated, dominant-negative CCAAT/enhancer-binding protein beta isoform and up-regulation of the eukaryotic translation initiation factor 2alpha are correlated with neoplastic transformation of mammary epithelial cells. Cancer Res 1996;56:4382–4386.

37. Lovat PE, Corazzari M, Armstrong JL, *et al*. Increasing melanoma cell death using inhibitors of protein disulfide isomerases to abrogate survival responses to endoplasmic reticulum stress. Cancer Res 2008;68:5363–5369.

38. Huang S, Ingber DE. Shape-dependent control of cell growth, differentiation, and apoptosis: switching between attractors in cell regulatory networks. Exp Cell Res 2000;261:91–103.

39. Perez-Moreno M, Jamora C, Fuchs E. Sticky business: orchestrating cellular signals at adherens junctions. Cell 2003;112:535–548.

40. Lombaerts M, van Wezel T, Philippo K, *et al*. E-cadherin transcriptional downregulation by promoter methylation but not mutation is related to epithelial-to-mesenchymal transition in breast cancer cell lines. Br J Cancer 2006;94:661–671.

41. Baryshev M, Sargsyan E, Mkrtchian S. ERp29 is an essential endoplasmic reticulum factor regulating secretion of thyroglobulin. Biochem Biophys Res Commun 2006;340:617–624.

42. García-Higuera I, Manchado E, Dubus P, *et al*. Genomic stability and tumour suppression by the APC/C cofactor Cdh1. Nat Cell Biol 2008;10:802–811.

43. Coopman PJ, Mueller SC. The Syk tyrosine kinase: a new negative regulator in tumor growth and progression. Cancer Lett 2006;241:159–173.

44. Gondi CS, Lakka SS, Dinh DH, *et al*. Intraperitoneal injection of a hairpin RNA-expressing plasmid targeting urokinase-type plasminogen activator (uPA) receptor and uPA retards angiogenesis and inhibits intracranial tumor growth in nude mice. Clin Cancer Res 2007;13:4051–4060.

45. Lee EJ, Whang JH, Jeon NK, *et al*. The epidermal growth factor receptor tyrosine kinase inhibitor ZD1839 (Iressa) suppresses proliferation and invasion of human oral squamous carcinoma cells via p53 independent and MMP, uPAR dependent mechanism. Ann NY Acad Sci 2007;1095:113–128.

46. Li Q, Mattingly R. Restoration of E-cadherin cell-cell junctions requires both expression of E-cadherin and suppression of ERK MAP Kinase activation in Ras-transformed breast epithelial cells. Neoplasia 2008;10:1444–1458.

47. Vantaggiato C, Formentini I, Bondanza A, *et al*. ERK1 and ERK2 motogen-activated protein kinase affect Ras-dependent cell signaling differentially. J Biol 2006;5:14.